UV-laser-induced polymer ablation: The role of volatile species.

M. Himmelbauer*, N. Bityurin**, B. Luk'yanchuk***, N. Arnold*, and D. Bäuerle*

*) Angewandte Physik Institute, Johannes Kepler University, A-4040, Linz, Austria
**) Institute of Applied Physics, Russian Ac. Sci., 603600, Nizhny Novgorod, Russia
***) General Physics Institute, Russian Ac. Sci., 117942, Moscow, Russia

ABSTRACT

Single-shot laser ablation of polyimide has been investigated with UV Ar^+-laser radiation ($\lambda \approx 302$ nm) for pulse lengths between 140 ns and 5000 ns. The dependences of the ablation rate on laser pulse length and intensity were measured by means of an atomic force microscope (AFM). These data are compared with mass-loss measurements using a microbalance[1]. The experimental data are analyzed by taking into account both mass losses related to volatile product species and real material ablation.

1. INTRODUCTION

The mechanisms of UV laser ablation of polymers are still under discussion despite the numerous investigations devoted to this subject (for a review see[2]). Thermal models, which assume that ablation is microscopically a surface process similar to the laser evaporation of metals, lead to an unrealistically high activation energies for ablation (close to covalent bond energies, i.e., typically ~3 to 5 eV[3,4]). Recent ablation experiments using a microbalance technique[1] reveal for polyimide (PI) an activation energy of about ~1 eV. An interpretation of such low activation energies has been given in[5-7] where a photophysical mechanism of laser ablation has been proposed. This model takes into account the thermal desorption of electronically excited species. However, low apparent activation energies can also be interpreted by considering both mass losses related to the elimination of volatile species formed by photodegradation within the bulk material and real ablation. In our experiments the dependences of the ablation threshold and the ablation rate on laser pulse length and intensity were analyzed by means of an atomic force microscope (AFM). The results are compared with mass-loss measurements using a microbalance[1].

2. EXPERIMENTAL

The polyimide foils (Kapton H, Du Pont, 50 μm thick) employed in the experiments were irradiated in air by an externally pulsed cw-Ar^+-laser (Spectra Physics) operating in the UV-region (TEM_{00} mode). With all experiments, the plasma current in the laser tube was kept constant to avoid changes in spot size and spectral distribution. The latter shows a pronounced maximum at a center wavelength λ_c=302 nm ($\Delta\lambda$ = 9 nm) and a less intense peak at around 275 nm. Rectangular laser pulses with pulse lengths τ_l = 140 ns - 5 μs at FWHM were generated by a digitally driven acousto-optic modulator (A.A. Opto-Electronique). Here, the cw-laser beam was focused into the quartz crystal ($2w_0(1/e) \approx 360$ μm), passed the acoustic-wave-induced gratings and was diffracted into several orders. The first order was selected by a pinhole and then focused onto the polymer surface. The focal size, measured by the scanning knife-edge technique, was $2w_0 = (4.2 \pm 0.4)$ μm [8]. The laser power was determined with a UV-photodiode which was calibrated by means of a disc calorimeter to an accuracy of about ±5%. Thin platelets of fused silica inserted into the optical path allowed one to change the laser power. The fluence on the polymer surface was of Gaussian shape, $\phi(r)=\phi_0 \exp(-(r/w_0)^2)$. Irradiated polymer foils were ultrasonically cleaned in acetone, in order to remove debris. The surface topology of the sample was then investigated by means of an atomic force microscope (Digital Instruments, Nanoscope III). In the contact mode, which was mainly employed, the sample was traced with a piezo-scanner (lateral scan size 125×125 μm) under the silicon-nitride cantilever with an integral tip (square pyramidal, 20-50 nm radius of curvature, 70° interior angle) while the distance between the sample surface and the tip was constant. In the present paper, we report on the analysis of the ablated depth, Δh. The topology of the irradiated surface will be discussed elsewhere [9].

SPIE Vol. 3093 • 0277-786X/97/$10.00

3. THE MODEL

The simplest ansatz that takes into account volatile product species thermally generated within the bulk material can be written as (the coordinate system is fixed with the ablation front)

$$\frac{\partial N_l}{\partial t} = v\frac{\partial N_l}{\partial z} + k_l\left(N_{0l} - N_l\right)\exp(-\Delta E_l / k_B T) \quad , \tag{1}$$

$$\frac{\partial I}{\partial z} = -\alpha I \quad , \tag{2}$$

$$\frac{\partial T}{\partial t} = v\frac{\partial T}{\partial z} + D_T\frac{\partial^2 T}{\partial z^2} + \frac{I\alpha}{c_p\rho} \tag{3}$$

The ablation velocity $v=v(t)$ can be described by

$$v = v_A \exp(-\Delta E_A / k_B T_s) \tag{4}$$

The boundary conditions are

$$\kappa\frac{\partial T}{\partial z}\Big|_{z=0} = \rho v \Delta H \tag{5}$$

$$I\big|_{z=0} = I_0(t)\exp\left[-\alpha_p\int_0^t v(t_1)dt_1\right], \quad N_l\big|_{z\to\infty} = 0\,,\ T\big|_{z\to\infty} = T_\infty \tag{6}$$

The initial conditions are

$$N_l\big|_{t=0} = 0, \quad T\big|_{t=0} = T_\infty\,. \tag{7}$$

Here, I is the light intensity, N_l the concentration of volatile species which are produced within the bulk material and ΔE_l the activation energy of the bulk reaction. k_l is a preexponential factor, T the temperature, $\kappa = D_T c_p\rho$ thermal conductivity, D_T the thermal diffusivity, and ΔH the apparent transition enthalpy which enters boundary condition (5). The boundary condition for the intensity considers the shielding of the incident light by the ablated products. α_p is the absorption coefficient within the plume recalculated to the depth of the ablated material. $I_0(t)$ describes the incident laser pulse shape.

In (1)-(6) we do not take into account the diffusion of small species during ablation. Immediately after ablation, the small species shall leave the polymer. The recalculated ablation depth Δh_{rec} can then be found from the total mass loss

$$\Delta M \equiv \rho\Delta h_{rec} = \rho\int_0^\infty v dt + m\int_0^\infty N_l(x,\infty)dx \tag{8}$$

Here, m is the average mass loss per (gaseous) molecule, while $\int_0^\infty v dt$ describes the real ablated depth. The last term is the mass loss which is not connected with the ablation itself.

The small species being trapped in the material produce a hydrostatic pressure

$$p \propto N_l T \tag{9}$$

The influence of this internal pressure on the activation energy for ablation can be described by:

$$\Delta E_A(p) = \Delta E_A - \gamma p \tag{10}$$

Thus, if we substitute (10) in (4) taking β to be the proportionality coefficient in (9), we obtain:

$$v = v_A \exp(\tilde{\gamma} N_l) \exp(-\Delta E_A / k_B T_s) \tag{11}$$

Here $\tilde{\gamma} = \gamma\beta / k_B$. In the calculations presented below we assumed $\tilde{\gamma} = 0$.

4. RESULTS AND DISCUSSION

Figure 1 exhibits the experimental data on mass loss measurements with PI using 308 nm XeCl laser radiation[1]. These data are fitted by the solution of eqs. (1)-(7). The solid curve represents the recalculated thickness, which corresponds to the overall mass loss described by (8). The dashed curve shows the mass loss associated with the elimination of volatile species, and it is described by the second term in (8). The dotted curve corresponds to real *ablation* and it is described by the first term in (8). At low fluences *all* mass loss can be attributed to the elimination of small molecules without real ablation. Ablation becomes significant only at higher fluences and it has a higher activation energy. The parameters used in the fit, are listed in the Table 1.

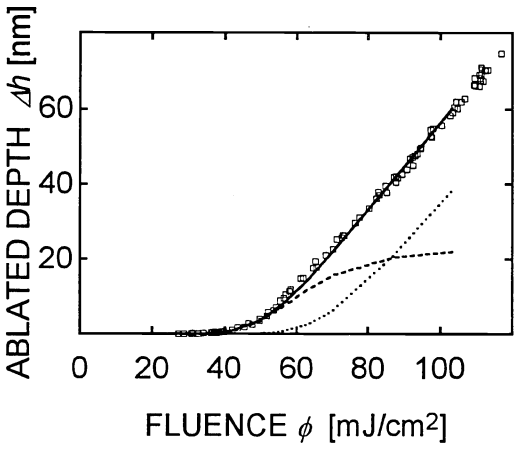

Figure 1: Ablated depth recalculated from the *mass loss*. Squares--experimental points[1]. Curves--theoretical calculations based on eqs. (1)-(7). Solid line--*total mass loss*, dashed line--mass loss due to volatile species, dotted line--mass loss due to real ablation. PI (Kapton H) ablated in *vacuum*, by XeCl laser at 308 nm. Parameters employed in calculations are listed in Table 1.

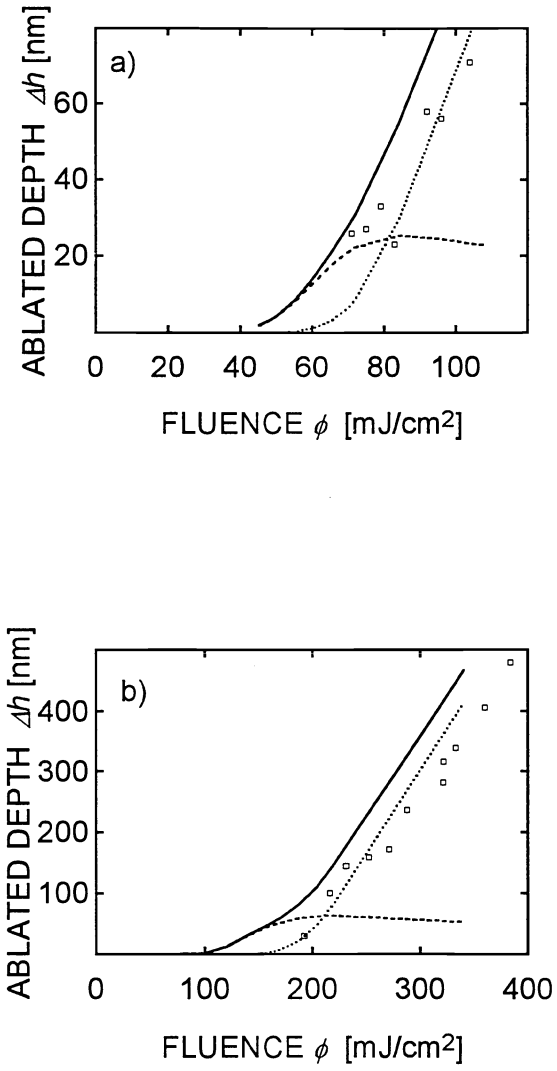

Figure 2: Squares--experimental points obtained by AFM measurements of the *ablated profile*[8]. Curves--theoretical calculations. Solid line--total mass loss, dashed line--mass loss due to volatile species, dotted line--mass loss due to *real ablation*. PI (Kapton H) ablated in *air*, Ar^+ laser at around 302 nm. a). τ_l=140 ns, b) τ_l=2000 ns.

In Fig. 2a,b the experimental data on the ablation of PI using Ar^+ - laser radiation ($\lambda \approx 302$ nm) and pulse lengths 140 ns and 2000 ns are displayed. Similar picture holds for pulse lengths up to 5000 ns. The ablated depth was measured by an AFM. The theoretical curves have been calculated from (1) - (7). It can be seen that the dotted curve fits the experimental data reasonably well for these pulse lengths. It is worth noting that we used here *the same parameters* as for the curves in Fig. 1, except of the absorption coefficient α and the enthalpy ΔH. Here we take into account that the absorption coefficient at 302 nm, α_{302}, is significantly higher than that at 308 nm, α_{308} [10,11]. We have used $\alpha_{302}=1.5\alpha_{308}$. For fitting data which are displayed in Fig. 2 we used $\Delta H=0$, while for Fig. 1 ΔH was taken to be 3.3×10^3 J/g. This difference may be related to the fact that the irradiation by Ar^+ laser was carried out in air. Oxidation may drastically change the mechanism of chemical degradation of PI during (slow) heating[12]. In our case, if the oxidation were essentially involved in material *removal* process,

we would obtain the changes in activation energy. However, in reality, we had to decrease not the activation energy, but the apparent transition enthalpy in (5). This latter decrease may be related to the post-oxidation *within the plume* which leads to an additional heating of the surface.

	XeCl λ=308 nm	Ar^+ λ=302±4.5 nm
ΔE_A, eV	2.75	2.75
ΔE_l^*, eV	1.47	1.47
v_A, cm/s	1.5×10^6	1.5×10^6
k_l^*, cm/s	2.24×10^{10}	2.24×10^{10}
ΔH, J/g	3.3×10^3	0
α, cm^{-1}	8.6×10^4	1.26×10^5
α_p, cm^{-1}	1.035×10^5	0
c_p, J/g·K	1.1	1.1
ρ, g/cm^3	1.42	1.42
D_T, cm^2/s	0.001	0.001
N_{0l}, cm^{-3}	6×10^{21}	6×10^{21}
T_∞, K	300	300

Table 1. The values of parameters used in the calculations.

It should be noted that we do not take into account any temperature dependences of parameters. Actually, the real temperature dependences are unknown for temperatures above 1000 K, because the material decomposes. Temperature dependences in parameters may change the values of fit parameters such as the activation energies and enthalpies. The corresponding analysis is the prospect of the forthcoming research.

5. CONCLUSIONS

The comparison of data on single-shot laser ablation measured by AFM and by microbalance techniques reveals two regimes of mass losses: With $\phi < \phi_{th}$ no real ablation takes place and the mass loss is determined by the desorption of small volatile fragments generated near the surface of the bulk material. Real ablation is observed only above a certain threshold fluence ϕ_{th} which can be determined with high accuracy by means of an AFM. These observations can be interpreted by a new model of polymer ablation which considers both channels - the elimination of volatile product species and real material removal. The present model describes the mass loss experiments and AFM experiments using almost the same set of parameters. The differences in transition enthalpy can be interpreted by the (exothermic) oxidation reaction within the plume.

6. ACKNOWLEDGMENTS

This work was supported in part by the Grant INTAS-94-902 and by the "Fonds zur Förderung der Wissenschaftlichen Forschung in Österreich".

7. REFERENCES

1. S. Küper, J. Brannon, K. Brannon, Appl. Phys. A **56**, 43, 1993.
2. D. Bäuerle, *Laser Processing and Chemistry*, Springer, Berlin, 1996
3. R. Srinivasan: In *Interaction of Laser Radiation with Organic Polymers*, Ed. by J. C. Miller, Springer Series in Materials Science **28**, Springer-Verlag, 1994, 107; R. Srinivasan, *Appl. Phys. A* **56**, 417, 1993
4. S. R. Cain, F. C. Burns, C. E. Otis, B. Braren: *J. Appl. Phys.* **72**, 5172, 1993
5. B. Luk'yanchuk, N. Bityurin, S. Anisimov, and D. Bäuerle: *Appl. Phys. A* **57**, 367 1993
6. B. Luk'yanchuk, N. Bityurin, S. Anisimov, and D. Bäuerle: *Appl. Phys. A* **57**, 449, 1993
7. B. Luk'yanchuk, N. Bityurin, S. Anisimov, N. Arnold, and D. Bäuerle: *Appl. Phys. A* **62**, 397, 1996
8. M. Himmelbauer, E. Arenholz, D. Bäuerle, and K. Schilcher: to appear in *Appl. Phys. A* **63**, 1996
9. M. Himmelbauer, E. Arenholz, and D. Bäuerle: to appear in *Appl. Phys. A* **63**, 1996
10. E. T. Arakawa, M. W. Williams, J. C. Ashley, and L. R. Painter, *J. Appl. Phys.* **52**, 3579, 1981
11. E. Sutcliffe, R. Srinivasan, *J. Appl. Phys.* **60**, 3315, 1986
12. M. I. Bessonov, *Polyimides - a Class of Thermally stable Polymers*, NASA Technical Memorandum, Washington DC 20546, 1986, (Translated from Russian: M. I. Bessonov, *Poliimidy - Klass Termostoikikh Polimerov,* Nauka, Leningrad, 1983)